

Taxus chinensis-Derived Nanovesicles Alleviate Mouse Colitis by Inhibiting Inflammatory Cytokines and Restoring Gut Microbiota

Qianyuan Gong^{1,*}, Junqing Hu^{2,3,*}, Chunlan Pu¹, Zihao Zhao¹, Yuanbiao Guo¹

¹Medical Research Center, The Affiliated Hospital of Southwest Jiaotong University, The Third People's Hospital of Chengdu, Chengdu, Sichuan, 610031, People's Republic of China; ²Obesity and Metabolism Medicine-Engineering Integration Laboratory, Department of General Surgery, The Affiliated Hospital of Southwest Jiaotong University, The Third People's Hospital of Chengdu, Chengdu, Sichuan, 610031, People's Republic of China; ³The Center for Obesity and Metabolic Health, Department of General Surgery, The Affiliated Hospital of Southwest Jiaotong University, The Third People's Hospital of Chengdu, Chengdu, Sichuan, 610031, People's Republic of China

*These authors contributed equally to this work

Correspondence: Qianyuan Gong, Email gqyscu@sina.cn

Background: Recent research has increasingly focused on plant-derived products as potential alternatives to chemotherapeutic agents, aiming to reduce side effects. Among these, plant-derived nanovesicles (NVs) have garnered significant attention for their potential in treating colitis.

Methods: In this study, we extracted NVs from the leaves (LNVs) and stems (SNVs) of *Taxus*, a well-known natural anti-cancer plant. The targeting ability of these NVs was evaluated in the mouse colon using an IVIS imaging system. Additionally, we assessed the therapeutic effects of these plant-derived NVs on ulcerative colitis in a mouse model.

Results: Our findings reveal that the NVs exhibit an ideal vesicle size of 150.0 nm and contain a rich array of lipids, functional proteins, and bioactive small molecules. In vitro anti-inflammatory experiments demonstrated that both LNVs and SNVs enhanced cell viability and reduced levels of pro-inflammatory cytokines. Importantly, neither LNVs nor SNVs induced significant cytotoxicity. In vivo, oral administration of LNVs and SNVs ameliorated colitis-related symptoms in mice and accelerated colitis resolution by suppressing the TLR4/MyD88/NF- κ B pathway and reducing levels of pro-inflammatory cytokines, including IL-1 β , IL-6, and TNF- α . Furthermore, 16S rDNA sequencing data suggested that LNVs play a crucial role in regulating gut microbiota.

Conclusion: Collectively, our findings suggest that plant-derived NVs from *Taxus* represent a promising novel natural nanomedicine for use as an anti-inflammatory agent in the treatment of colonic diseases.

Keywords: colitis, plant-derived nanovesicles, gut microbiota

Introduction

Ulcerative colitis (UC) is a chronic inflammatory condition affecting the colon and rectum, characterized by mucosal and submucosal inflammation.¹ Despite extensive research, the precise etiology of UC remains elusive. Common symptoms include diarrhea, weight loss, rectal bleeding, and dysbiosis of the gut microbiota.² Current therapeutic strategies primarily involve immunosuppressants, amino-salicylic acid derivatives, and biologics, which, while effective, are often associated with significant adverse effects such as allergic reactions, nausea, and hepatotoxicity.^{3,4} These limitations underscore the urgent need for safer and more effective treatment options.

Recent advancements in drug delivery systems have highlighted the potential of nanoparticles with colon-targeting capabilities for UC therapy.⁵⁻⁷ However, concerns regarding biosafety and the high cost of large-scale production have hindered their clinical application.⁸ In this context, nanovesicles (NVs) derived from natural sources have emerged as promising candidates.^{9,10} These NVs are rich in bioactive molecules, exhibit excellent biosafety profiles, and can be produced on a large scale.¹¹ Notably, plant-derived NVs have shown the ability to interact with mammalian cells,

particularly intestinal macrophages, and exert diverse biological effects depending on their plant origin.^{12–18} This has led to the exploration of plants as nano-factories for the production of therapeutic NVs, offering a novel platform for disease treatment.

Taxus, a globally endangered tree species, is renowned for its bark, which contains paclitaxel, a potent anticancer compound.¹⁹ Paclitaxel is widely used in the treatment of various cancers, including breast, lung, and ovarian cancer.^{20,21} However, the limited availability of paclitaxel in *Taxus chinensis* (*T. chinensis*) bark has prompted the search for additional bioactive compounds within this species.^{22–24} Recent studies have identified a variety of antimicrobial, antioxidant, and anticancer metabolites in *T. chinensis*, such as dodecanol, phosphomycin, L-malic acid, tartaric acid, 2,3-dihydroxybenzoic acid, and salicin.^{25–31} Despite these findings, the potential effects and mechanisms of *T. chinensis* on colitis remain poorly understood.

In this study, we hypothesize that orally administered *T. chinensis*-derived NVs (TcNVs) may exert therapeutic effects on UC. We aim to investigate the anti-inflammatory properties of TcNVs both in vitro and in vivo, focusing on their impact on UC symptoms, colonic phenotype, disease activity index, histopathology, pro-inflammatory cytokine expression, and gut microbiota composition. Our findings may provide new insights into the development of natural nanomedicines for the treatment of colonic diseases.

Materials and Methods

Chemicals and Reagents

Fresh leaves and stems of *T. chinensis* were collected from the botanical garden, located in Chengdu University of Traditional Chinese Medicine (Chengdu, China) and the plant materials were identified by Professor Yuntong Ma from Chengdu University of Chinese Medicine and stored in the Herbarium of Chengdu University of Chinese Medicine (No. 511113200508236LY). Sucrose was provided from Sangon Biotech (Shanghai, China). All cell culture reagents, including RPMI 1640 medium, fetal bovine serum (FBS), Penicillin/Streptomycin, were purchased from Gibco. Phosphate buffered saline (PBS) and 4% paraformaldehyde were purchased from Biosharp (Hefei, China). 1,1-Dioctadecyl-3,3,3,3-tetramethylindotricarbocyanine iodide (DiR) was obtained from AAT Bioquest (Pleasanton, USA). Phalloidin-FITC was purchased from Abcam. 4',6'-Diamidino-2-phenylindole (DAPI), Alexa Fluor 488 and 594 were purchased from Solarbio (Beijing, China). Lipopolysaccharide (LPS) and phorbol 12-myristate 13-acetate (PMA) were provided by Sigma-Aldrich. Dextran Sulfate Sodium Salt (DSS, 36000–50000 Da, colitis grade) was obtained from MP Biomedicals. The Cell Counting Kit-8 (CCK-8) and RIPA buffer were obtained from Beyotime (Beijing, China). Trizol was purchased from TianGen (Beijing, China), M-MLV reverse transcriptase and SYBR quantitative PCR Mix were provided from Vazyme (Nanjing, China). The bicinchoninic acid (BCA) protein assay kit was obtained from Thermo Fisher Scientific. TLR4, β -ACTIN, and MyD88 primary antibodies were purchased from Proteintech (Wuhan, China). The antibody of p-NF- κ B-p65 was obtained from Cell Signaling Technology (Danvers, USA). PVDF membrane and chemiluminescence reagent were purchased from Millipore (Massachusetts, USA). ELISA kits (mouse TNF- α , IL-1 β , IL-6, ALT, AST) were provided by Neobioscience (Shenzhen, China).

Isolation and Purification of TcNVs

Fresh leaves and stems of *T. chinensis* (10 g) were placed into 50 mL PBS and homogenized in a blender. The resulting juice was centrifuged at $1000 \times g$, $3000 \times g$, and $10,000 \times g$ for 10, 20, and 30 min, respectively. The supernatant was filtered at $0.45 \mu\text{m}$ to remove large particles of fibers and tissue. Subsequently, NVs were isolated by centrifuged at $100,000 \times g$ for 3 h and purified on a discontinuously sucrose gradient (8%, 15%, 30%, 45%). NVs from 30/45% interface were harvested, and BCA was used to determine the protein concentration. NVs were stored at -80°C .

Compositional Analysis of TcNVs

For TcNVs lipids composition analysis, total lipids of TcNVs were extracted by methyl tert-butyl ether/methanol (3:1, v/v) mixed solvent, and the lipidomic analysis of TcNVs was performed using triple quadrupole-linear ion trap mass spectrometer (Applied Biosystems, Foster City, USA).

For proteomics analysis, TcNVs were shipped to Duolaimi Biotechnology Co., Ltd. on dry ice. Proteins in TcNVs were analyzed by liquid chromatography-tandem mass-spectrometry. Briefly, the sample was separated on Easy-nLC chromatographic system. The elution program was as follows: 0–50 min, the rate of buffer solution B (acetonitrile: formic acid = 800:1, v/v) ranging from 8% to 95%. The isolated proteins were then subjected to data-independent acquisition mass spectrometry analysis.

Biodistribution Study of TcNVs

Oral administration of DiR-labeled TcNVs (1 mg protein/kg) was given to the healthy mice for 2 h. Then, the distribution of TcNVs was captured by the IVIS Lumina LT Series III (PerkinElmer, Hopkinton, USA). Subsequently, the mice were killed, and their gastrointestinal tissues were excised for imaging.

In vitro Anti-Inflammatory Activity of TcNVs

THP-1 monocyte cells (National Collection of Authenticated Cell Cultures, Serial No. SCSP-567) (2×10^4 cell/well or 5×10^5 cell/well) were seeded in 96-well plates or 6-well plates (Corning, Kennebunk, USA) and differentiated into macrophages by 100 ng/mL PMA treatment for 24 h. Then, the cells were stimulated with 2 µg/mL LPS and different concentrations of NVs for 24 h. The cell vitality was tested by CCK-8 and the expression of inflammation-related genes were analyzed using RT-qPCR.

Reverse Transcription-quantitative (RT-q) PCR Assays

Total RNA was extracted from the cell with Trizol, and 1 µg of RNA was used for reverse transcription and the gene expression was quantified by SYBR qPCR machine (Roche, Rotkreuz, Switzerland). The following conditions were used: 94°C for 2 min, followed by 40 cycles at 94°C for 20 s and 60°C for 30 s. Primers used are shown in [Table S1](#).

Animal Experiments

C57BL/6J mice (male, 8 weeks, 18–22 g) were purchased from Dossy Experimental Animal Ltd. (Chengdu, China) and housed under a 12-hour dark/light cycle at 25 °C and 50% humidity. All mice were adapted feeding for 7 days, and then randomly divided into four groups: negative control, positive control, LNVs and SNVs groups (n = 8 per group). Mice in the LNVs and SNVs groups were administered with NVs (1 mg/kg/day) by gavage for 17 days. Between days 8 and 17, mice in the positive control, LNVs and SNVs groups received 2% DSS in their drinking water. UC-related symptoms, including body weight, stool consistency, and fecal bleeding, were recorded daily. On the 17th day, all mice were sacrificed and the colon tissue, blood, and colonic contents were collected. About 1 cm colons were fixed in 4% paraformaldehyde and paraffin sections (4 µm thickness) and used for histological assessment by hematoxylin and eosin (H&E). Colonic content samples were snap frozen at –80 °C after collection.

Western Blotting

Total proteins from colon tissue were lysed in RIPA buffer for 20 min. Protein concentration was measured by BCA and separated by SDS-PAGE and then transferred to a PVDF membrane at 80 V for 2 h. Blots were incubated with TLR4, MyD88, p-NF-κB-p65 antibody (1:1000) and anti-β-ACTIN (1:5000) overnight at 4 °C. Blots were incubated with a secondary antibody (horseradish peroxidase-conjugated) for 1 hour at room temperature and then chemiluminescence reagent was used to detect the proteins.

16S rDNA Gene Sequencing

Microbial DNA was extracted from the colonic contents using the DNeasy PowerSoil kit (Qiagen, Hilden, Germany). The quality of the isolated DNA was checked using 1.5% agarose gel electrophoresis. Universal primer couples were used to amplify the V3–V4 segment of the ribosomal DNA (16S) gene from bacteria (798R: 5'-AGGGTATCTAATCCT-3'; 343F: 5'-TACGGRAGGCAGCAG-3'). The PCR products were purified with AMPure beads (Beckman, California, USA). After adjusting the concentrations, sequencing was completed by OE Biotech Company (Shanghai, China).

Bioinformatic Analysis

The first step in processing raw paired-end reads is performed using Cutadapt software; this involves identifying and removing the adapter sequence. Then, reads were processed using DADA2 with QIIME2 to filter low-quality sequences.³² At last, the representative reads and the amplicon sequence variant (ASV) abundance table were generated. All representative reads were assigned against Silva 138 database using q2-feature-classifier with the default parameters. The microbial alpha diversity in colonic content samples was estimated using the ASV table including Observed ASVs, Shannon index, and PD whole tree indices. The beta diversity distance matrix Jaccard was constructed by QIIME2 and was used for Principal coordinates analysis (PCoA).

Statistical Analysis

All biochemical and host data were analyzed using OriginLab Corporation 9.0 and IBM SPSS Statistics software 25.0, and the data were presented as means \pm standard deviation (SD). The one-way ANOVA was used to compare the differences between groups, and P values greater than 0.05 were considered not significant. The R software was used to analyze the microbial significant differences between different groups using *T* test (pairwise comparisons with pooled SD) for alpha diversity, PERMANOVA for community structure, and Kruskal Wallis statistical test for composition data. Linear discriminant analysis (LEfSe) was used to compare the microbial taxonomic abundance spectrum. Spearman correlation was performed by “psych” package 1.9.12.31 in R 3.6.2.

Results

Characterization of TcNVs

To investigate NVs in the stems and leaves of *T. chinensis*, NVs from stems (SNVs) and leaves (LNVs) were extracted by differential centrifugation. Transmission electron microscope images revealed that SNVs and LNVs appeared circular and varied in size 100–200 nm (Figure 1A). The size distribution of SNVs and LNVs were measured by nanoparticle tracking analysis. The average diameter of SNVs and LNVs was 148.8 and 149.1 nm, consistent with transmission electron microscope results, and the concentration of SNVs and LNVs was 0.0314 mg/g and 0.0533 mg/g, respectively (Figure 1B).

Lipids compositional analysis showed that TcNVs were mainly comprised of triacylglycerol (TG), phosphatidylethanolamine (PE), diacylglycerol (DG), phosphatidylcholine (PC), and monogalactosyldiacylglycerol (MGDG) (Figure 1C and Table S2). Based on the present liposome delivery system, these lipids in TcNVs largely promote the formation of nanovesicles and maintain their spherical structure. For example, PE, PC, phosphatidylcholine (PA), and other phospholipids constitute the essential components of liposome lipid bilayer.³³ MGDG has an important contribution to the stability of liposomes in low-temperature environment.³⁴

Next, protein composition analysis revealed that a series of membrane-related proteins, such as H⁺-exporting diphosphatase, lipid-transfer protein, tubulin alpha chain, murein transglycosylase, outer membrane lipoprotein I, and plasma membrane intrinsic protein, were found in TcNVs (Figure 1D and Table S3). These membrane-associated proteins likely contribute to vesicle stability and biological activity, thereby maintaining the nanovesicle-like properties of TcNVs.

Intestine and Cellular Uptake of TcNVs

To exert biological effects, it is necessary for NVs to transfer their molecular contents into the intestine in the treatment of UC.³⁵ We measured in vivo accumulation of oral DiI-labeled TcNVs in healthy mice. Compared with the control group, the fluorescence intensity of TcNVs in gastrointestinal tissues, especially in colon, was significantly enhanced (Figure 2). The data indicated that TcNVs can be targeted to accumulate in the colon to exert their biological activity.

We also tested whether TcNVs can be taken up by human cells. We treated THP-1 macrophage cells with DiI-labeled TcNVs. The data in Figure S1 revealed that the fluorescence intensity gradually increased in a time-dependent and concentration-dependent manner. Microscope analysis revealed that TcNVs were widely distributed throughout the cell cytosol and surrounding the nucleus, implying that TcNVs can be absorbed by human cells. Plant NVs can be specifically internalized by galactose receptor-mediated endocytosis (ligand–receptor interaction),³⁶ so TcNVs may also be absorbed by macrophages through the same internalization.

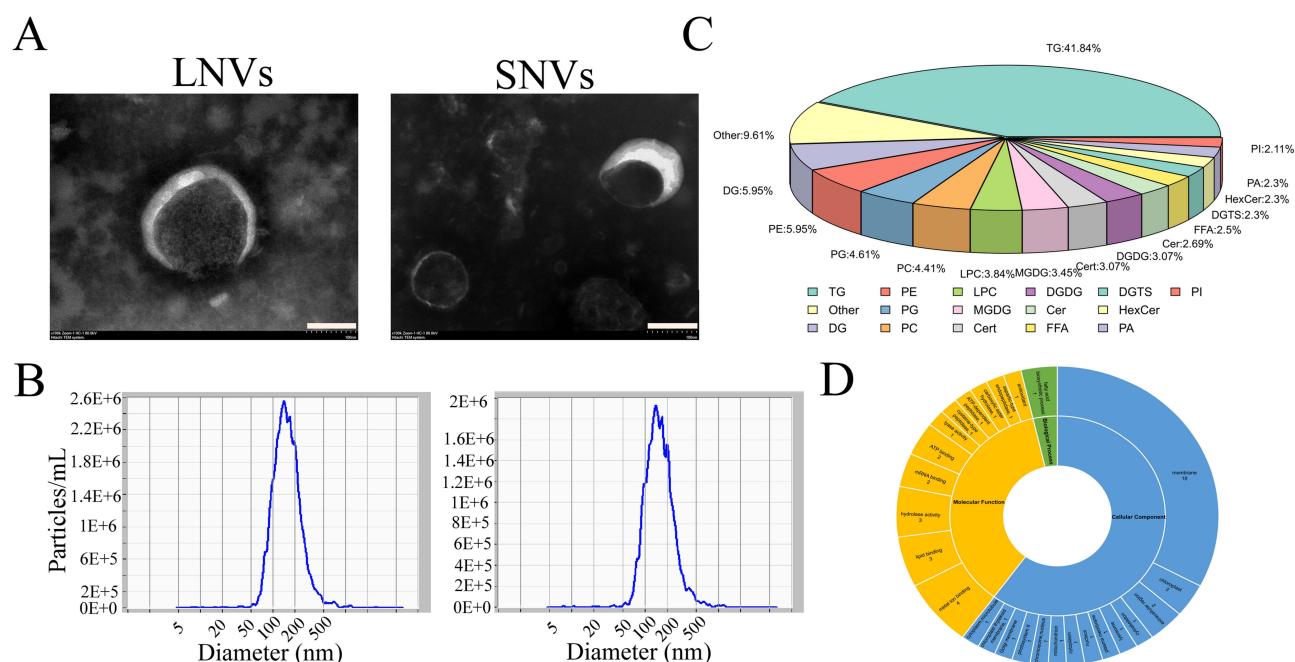


Figure 1 Characterization of TcNVs. **(A)** TcNVs were examined by transmission electron microscopy. Scale bar = 100 nm. Magnification: 120000X. **(B)** The particle size of TcNVs was analyzed by nanoparticle tracking analysis. **(C)** The lipid profiles of TcNVs under positive and negative mode. The lipid composition of TcNVs was determined by using a triple quadrupole mass spectrometer. The data are as percent ages of total signal for the molecular species determined after normalization of the signals in internal standards of the same lipid class. **(D)** The go secondary classification statistical charts of TcNVs.

Abbreviations: TG, triacylglycerol; PE, phosphatidylethanolamine; DG, diacylglycerol; PC, phosphatidylcholine; MGDG, monogalactosyldiacylglycerol; DGDG, digalactosyldiacylglycerol; PG, phosphatidylglycerol; PA, phosphatidic acid; LPC, lysophosphatidylcholine; PI, phosphatidylinositol; Cert, phytoceramide; FFA, free fatty acid; Cer, ceramide; DGTS, diacylglyceryl trimethylhomoserine; HexCer, hexosylceramide.

In vitro Anti-Inflammatory Activity of TcNVs

To clarify whether TcNVs have a regulatory effect on macrophages after ingestion by THP-1, we analyzed the effect of TcNVs on THP-1 proliferation. As shown in [Figure S2](#), different concentrations of TcNVs had no significant influence or toxic effect on the cell vitality of macrophages.

We then evaluated the anti-inflammatory effect in LPS-induced THP-1 cells. Notably, the SNVs and LNVs treatment significantly increased the cell vitality of THP-1 cells in a dose-dependent manner ([Figure 3A](#) and [B](#)). According to the anti-inflammatory experimental results, 10 $\mu\text{g/mL}$ TcNVs was considered to be the best concentration to enhance the anti-inflammatory effect of cells (cell viability was maintained about 90%). In addition, the SNVs and LNVs treatment suppressed the expression of inflammation cytokines IL-6, IL-8, IL-1 β , and TNF- α compared with the LPS treatment ([Figure 3C–F](#)). These results suggested that TcNVs have anti-inflammatory activity in LPS-induced macrophage cells.

Biosafety of TNVs in vivo

To assess the safety of orally administered TNVs, major organs (heart, liver, spleen, lung, and kidney) and serum sample were collected from mice that were administered 1 mg/kg TNVs for 17 days. Histological examination of the major organs by H&E staining revealed that there were no obvious signs of damage or abnormality in the organs of TNVs-treated mice ([Figure S3A](#)). In addition, there were no significant changes in ALT and AST levels between control and TNVs-treated mice ([Figure S3B](#)).

Retardation of UC Development by TcNVs

Based on these results, we next aim to investigate the effect of TcNVs on DSS-induced colitis, which is a well-established mouse model for studying UC in humans.^{37,38} Consistent with previous studies, the model mice exhibited varying degrees of diarrhea, weight loss, blood in the stool, and other colonic inflammation. Compared with the normal group, the colon length of mice in the model group was shortened ($P < 0.01$), the DAI scores of weight loss, bloody stool,

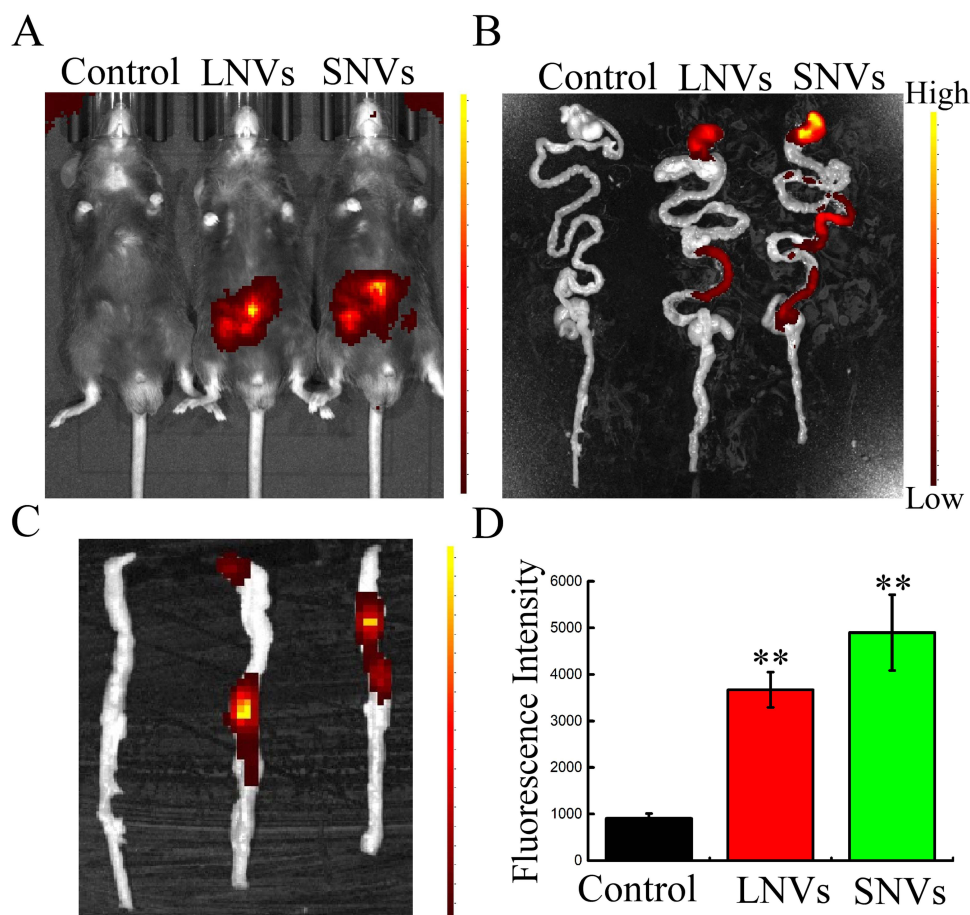


Figure 2 In vivo distribution of DiR-labeled TcNVs. (A) Whole body imaging of the mice (healthy, LNVs treated and SNVs treated) at 2 h after oral administration of DiR-labeled TcNVs (1 mg/kg) by IVIS Spectrum Series imaging system. (B) The distribution of DiR-labeled TcNVs in the gastrointestinal tract captured by the IVIS system at 2 h after gavage. (C) The distribution of DiR-labeled TcNVs in the distal colons captured by the IVIS system at 2 h after gavage. (D) The relative fluorescence intensity in (C) was quantified using Image J software. The lowercase letters above bars indicated significant differences by one-way ANOVA. Data are shown as the mean \pm SD (n=3). **p < 0.01 compared to the control group.

and diarrhea were significantly increased ($P < 0.01$) (Figure 4). Compared to the model group, SNVs and LNVs treatment group could improve the shortened colon in colitis mice ($P < 0.01$) (Figure 4D and E), and the DAI scores were significantly reduced in colitis mice ($P < 0.01, 0.05$) (Figure 4C). This suggests that TcNVs can effectively prevent colon damage in colitis mice.

Effects of TcNVs on the Pathological Changes of Colon Tissue in UC

The histological effects of TcNVs on colitis were evaluated by H&E staining (Figure 5A). DDS-treated mice exhibited increased mucosal damage and inflammatory cell infiltration, compared to the normal mice. However, mice treated with TcNVs showed decreased mucosal injury and inflammatory infiltrates. Further H&E staining scores of colon tissue showed that TcNVs treatment significantly decreased the score of colonics ($P < 0.01$) (Figure 5B).

Moreover, electron microscopy of epithelial cells in the colonic mucosa of mice demonstrated notable differences among the experimental groups. In comparison to the control group, the model group exhibited incomplete and partially damaged tight junctions between intestinal epithelial cells, along with a disrupted microvillus structure. Conversely, the TcNVs treatment group showed a tendency towards intact tight junctions, with no significant morphological damage observed (Figure S4). These findings suggest that TcNVs may effectively prevent and ameliorate intestinal barrier damage associated with colitis.

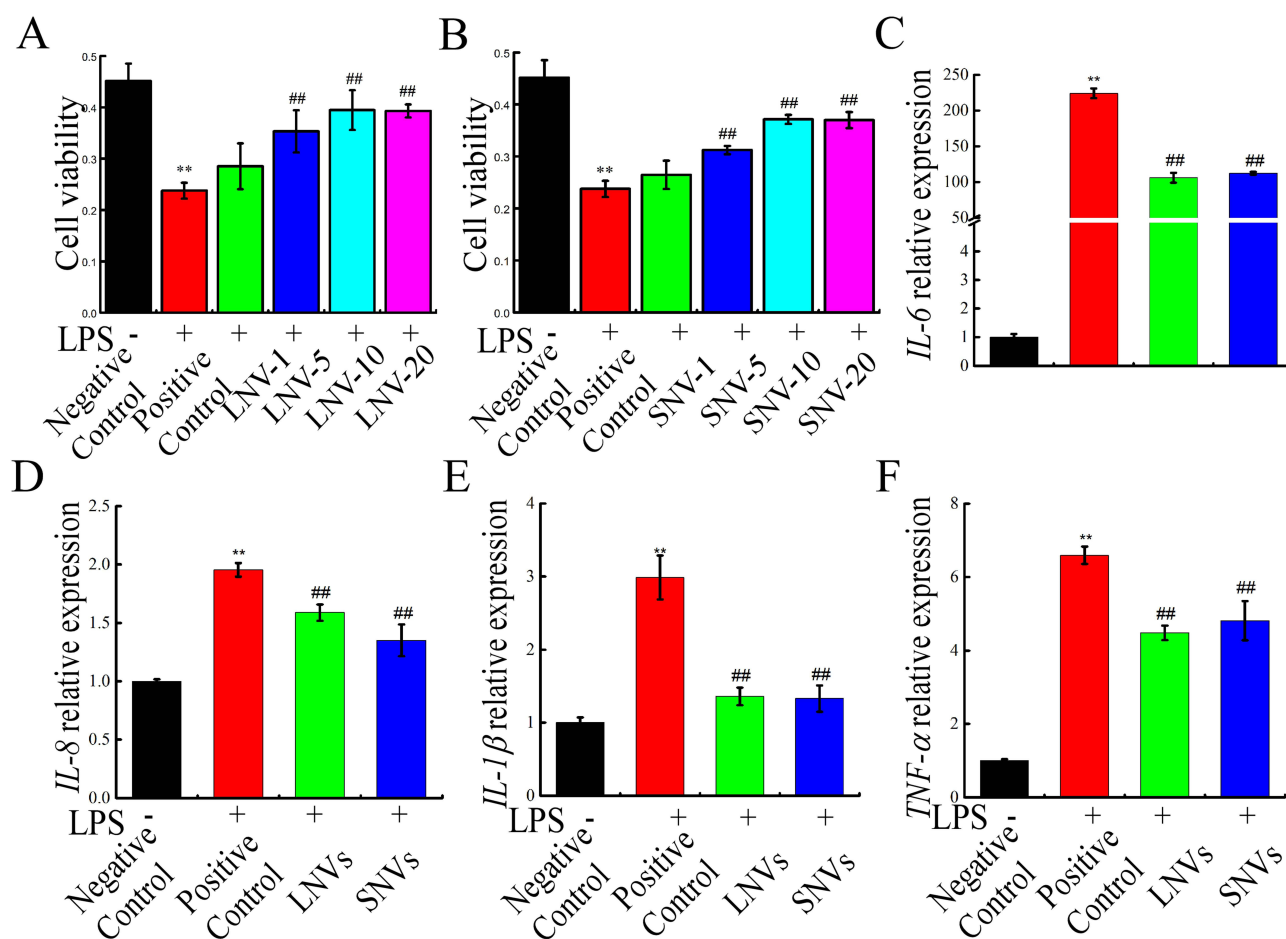


Figure 3 In vitro anti-inflammatory properties of TcNVs. (A and B) The LNVs (A) and SNVs (B) dose-dependently enhanced the cell vitality of LPS stimulated macrophages. Different amounts of TcNVs (1 μ g/5 μ g/10 μ g/20 μ g/mL, represented by SNV/LNV-1/5/10/20) were added to the THP-1 macrophages for 24 h. The cell vitality was tested by Cell Counting Kit-8. (C–F) Result of inflammation-related cytokine IL-6 (C), IL-8 (D), IL-1 β (E), and TNF- α (F) mRNA expression in LPS stimulated macrophages. Data are shown as the mean \pm SD (n=3). **p < 0.01 compared to the negative control group; ###p < 0.01 compared to the positive control group.

During UC development, neutrophils are usually activated at inflamed intestinal sites.³⁹ This process may be accompanied by an increase in the levels of pro-inflammatory cytokines (TNF- α , IL-6, and IL-1 β) in the model group compared to healthy mice (Figure 5C–E), while oral administration of TcNVs could decrease the secretion of these cytokines.

Effects of TcNVs on TLR4/MyD88/NF- κ B Inflammatory Pathway in UC

The toll-like receptor 4 (TLR4) and nuclear factor κ B (NF- κ B) constitute a crucial inflammatory signal transduction pathway in UC progression.⁴⁰ This pathway plays a pivotal role in mediating inflammatory responses and promoting the synthesis of pro-inflammatory cytokines, thereby exacerbating epithelial barrier dysfunction. DSS-treated mice significantly increased the expression levels of MyD88 and TLR4, as well as the phosphorylation levels of NF- κ B p65, compared to the normal mice (p < 0.05). Notably, the TcNVs treatment remarkably induced under-expression of MyD88 and TLR4, and the under-phosphorylation of NF- κ B p65 by 47%, 49%, and 79% (p < 0.05) compared to the model group, respectively (Figure 6A–D). Therefore, the anti-UC activity of TcNVs could be partly attributed to down-regulated the TLR4/MyD88/NF- κ B inflammatory pathway.

Effects of TcNVs on the Bacterial Composition and Community Structure of the UC Mice

The gut bacteria were analyzed by 16S rDNA sequencing to explore the enteric-origin mechanism of TcNVs against UC. Rank abundance and alpha diversity index analysis found that LNVs and SNVs had no significant influence on the gut

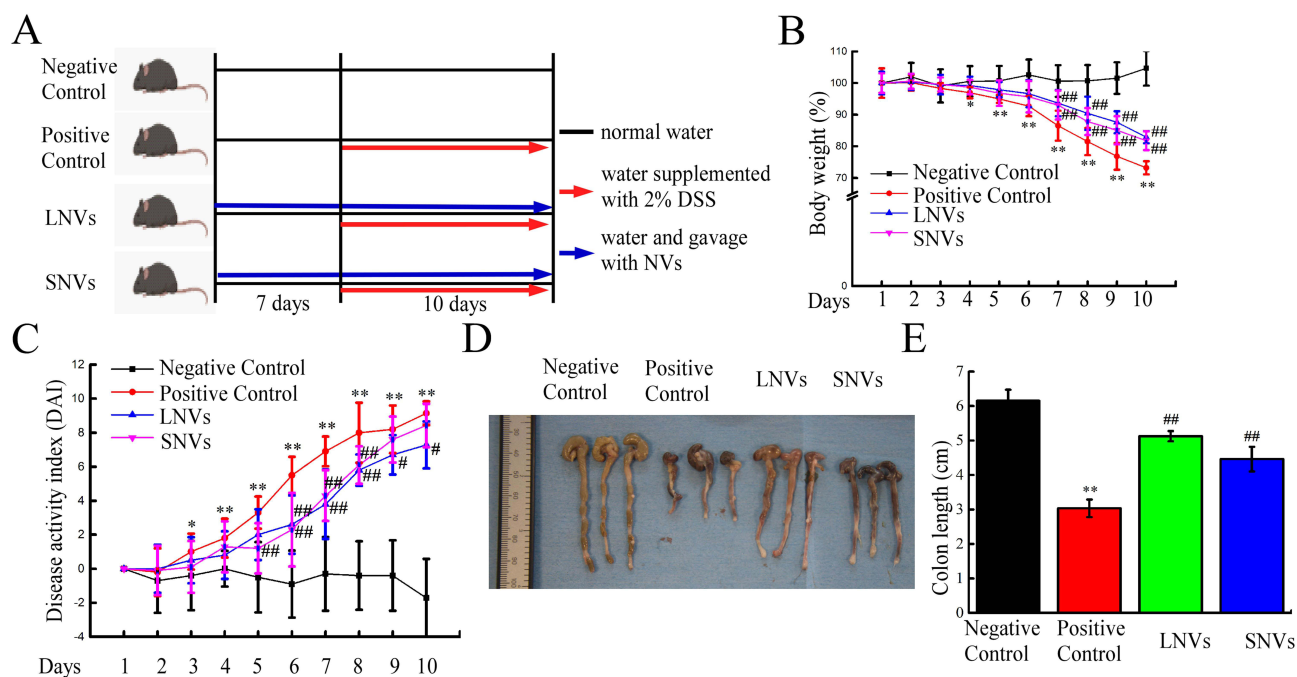


Figure 4 TcNVs ameliorated the progression of DSS-induced mice colitis. **(A)** Experimental design to test the effects of TcNVs on DSS-induced colitis in mice ($n = 8$ /group). **(B)** Result of body weight on TcNVs treatment in DSS-induced colitis. **(C)** Disease activity index (DAI) scores in each group. **(D)** Representative images of colon length in each group. **(E)** Statistical analysis of colon length in **(D)**. Data are shown as the mean \pm SD ($n=8$). ** $p < 0.01$ and * $p < 0.05$ compared to the negative control group; ### $p < 0.01$ and # $p < 0.05$ compared to the positive control group.

bacterial diversity (Figure S5). Thus, we focused on the changes in bacterial community structure, given that minor difference in diversity after TcNVs were applied in the current study. The number of intestinal bacterial ASV of mice in the negative control group, positive control group, LNVs group and SNVs group were 582, 285, 295, and 204, respectively (Figure 7A). At the phylum level, Firmicutes, Bacteroidota, Proteobacteria, Desulfobacterota, and Campilobacterota were the top five phyla (Figure 7B). At the genus level, *Muribaculaceae*, *Lachnospiraceae* NK4A136 group, *Bacteroides*, *Escherichia-Shigella*, *Parasutterella*, *Helicobacter*, *Mucispirillum*, *Colidextribacter*, *Odoribacter*, *Alistipes*, *Clostridia vadinBB60* group, *Lactobacillus*, *Lachnoclostridium*, *Rikenellaceae* RC9 gut group, and *Roseburia* were the dominant genera (Figure 7C). The PCoA analysis (Jaccard distance) showed that marked changes in gut community among the groups ($P = 0.001$) (Figure 7D).

Effects of TcNVs on the Taxonomic Biomarkers and Correlation with Host in the UC Mice

We further explored the biomarkers (significantly altered taxa) in the gut of DSS-induced UC mice after the TcNVs treatment by LEfSe analysis. Unexpectedly, *Escherichia coli*, a species from genus *Escherichia-Shigella*, was found to bloom in the LNVs group but was at a similar level in SNVs group with negative group (Figures S6A and 8A). Importantly, *Clostridiales bacterium* was significantly decreased after SNVs treatments and *uncultured bacterium* (*Lachnospiraceae* NK4A136 group) was increased in the positive control group, but decreased to similar level of that in the negative control group after LNVs and SNVs treatments (Figure S6B and C). Genera *Bacteroides*, *Butyricimonas*, *Dubosiella*, *Prevotellaceae_UCG_001*, and *Eubacterium_coprostanoligenes_group* were enriched in the SNVs group (Figure 8A).

We finally used Spearman's algorithm to analyze the correlation between DAI, inflammatory factors (IL-1 β , TNF- α , and IL-6), and the intestinal bacteria, including significantly enriched in LNVs and SNVs groups identified by LEfSe (Figure 8B). *Bacteroides* was significantly positively correlated with DAI (FDR < 0.001) and IL-6 (FDR < 0.05), while showed a significant negative correlation with body weight (FDR < 0.01) and colon length (FDR < 0.05). Conversely,

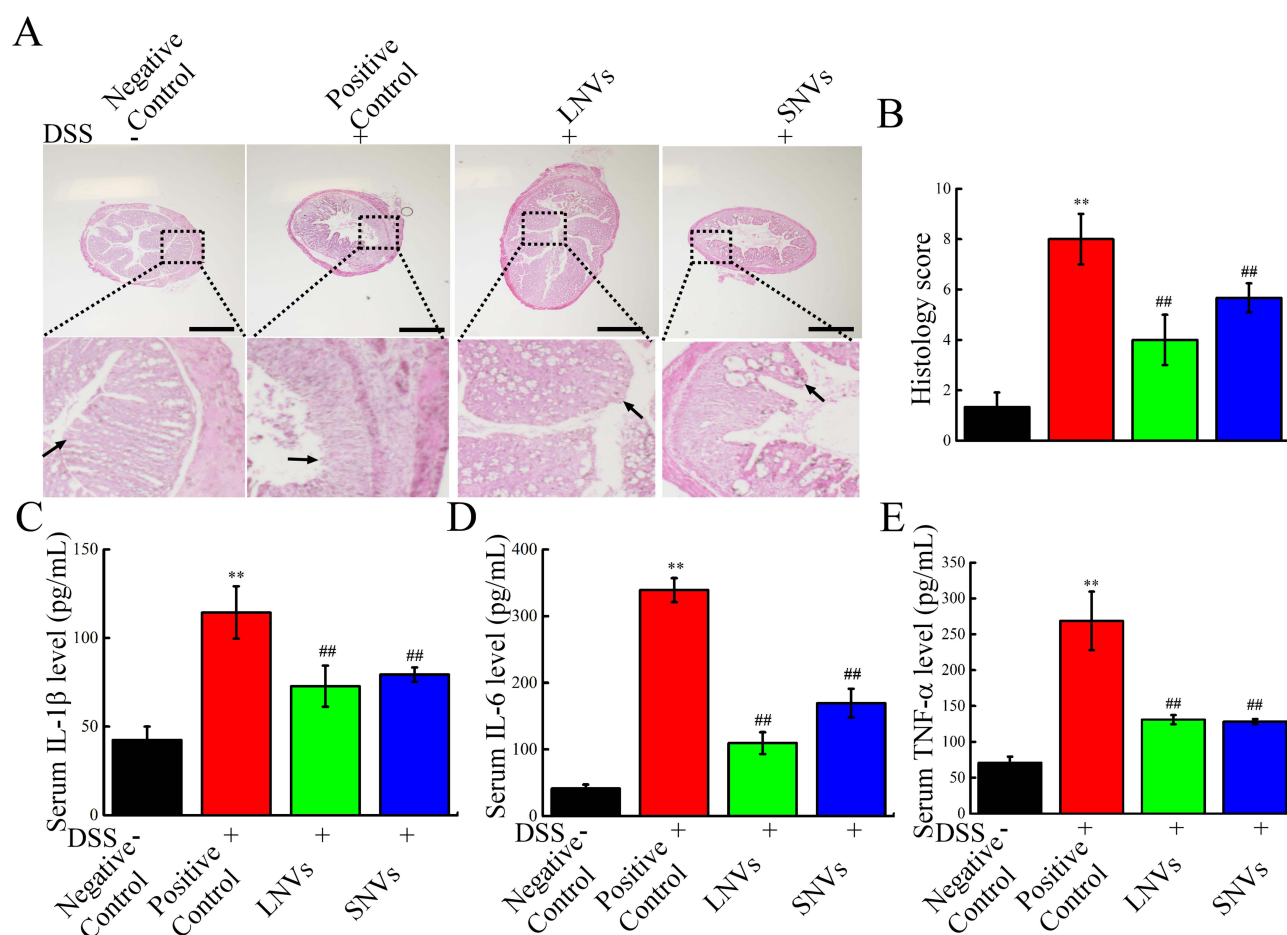


Figure 5 TcNVs treatment improved mucosal inflammation of colitis tissues. **(A and B)** Representative colon histological sections stained with hematoxylin and eosin (H&E). Scale bar = 200 μ m. **(C–E)** Result of IL-1 β , IL-6, and TNF- α in serum. Data are shown as the mean \pm SD (n=3). **p < 0.01 compared to the negative control group; ###p < 0.01 compared to the positive control group.

Muribaculaceae and Roseburia were significantly negatively correlated with DAI (FDR < 0.05) and IL-6 (FDR < 0.05), whereas they were positively correlated with body weight (FDR < 0.05) and colon length (FDR < 0.05). In addition, *Lactobacillus* and *Rikenella* were significantly negatively correlated with DAI (FDR < 0.05, 0.01), but markedly positively correlated with body weight (FDR < 0.05, 0.01).

Discussion

Nanoparticulate systems have drawn interest as potential treatments for colitis, because they possess unique physico-chemical properties and the ability to target disease sites.^{41,42} Nanovesicles (NVs) derived from plants have become a branch of nanomedicine due to their ability to inter-kingdom communicate between the animal and plant, and thus possess the potential for treating a variety of diseases, including UC.⁴³ Here, TcNVs were obtained from fresh *T. chinensis*, a natural anti-cancer plant in the world. The preparation process of TcNVs does not need to add any organic solvent and is easy for industrial large-scale production. Therefore, TcNVs may provide a safe and simple approach to UC therapy.

Plant-derived NVs have the function of targeting the colon. After oral administration of vesicles, a large concentration of vesicles can be detected in the colon or colon stem cells.^{13,14,44} In the diseased colonic site, NVs accumulation can exert anti-inflammatory activity by inducing the proliferation of intestinal stem cells and restoring the intestinal barrier (such as enhancing the expression of tight junction proteins such as ZO-1 and occludin).^{13,16,45} We also found that

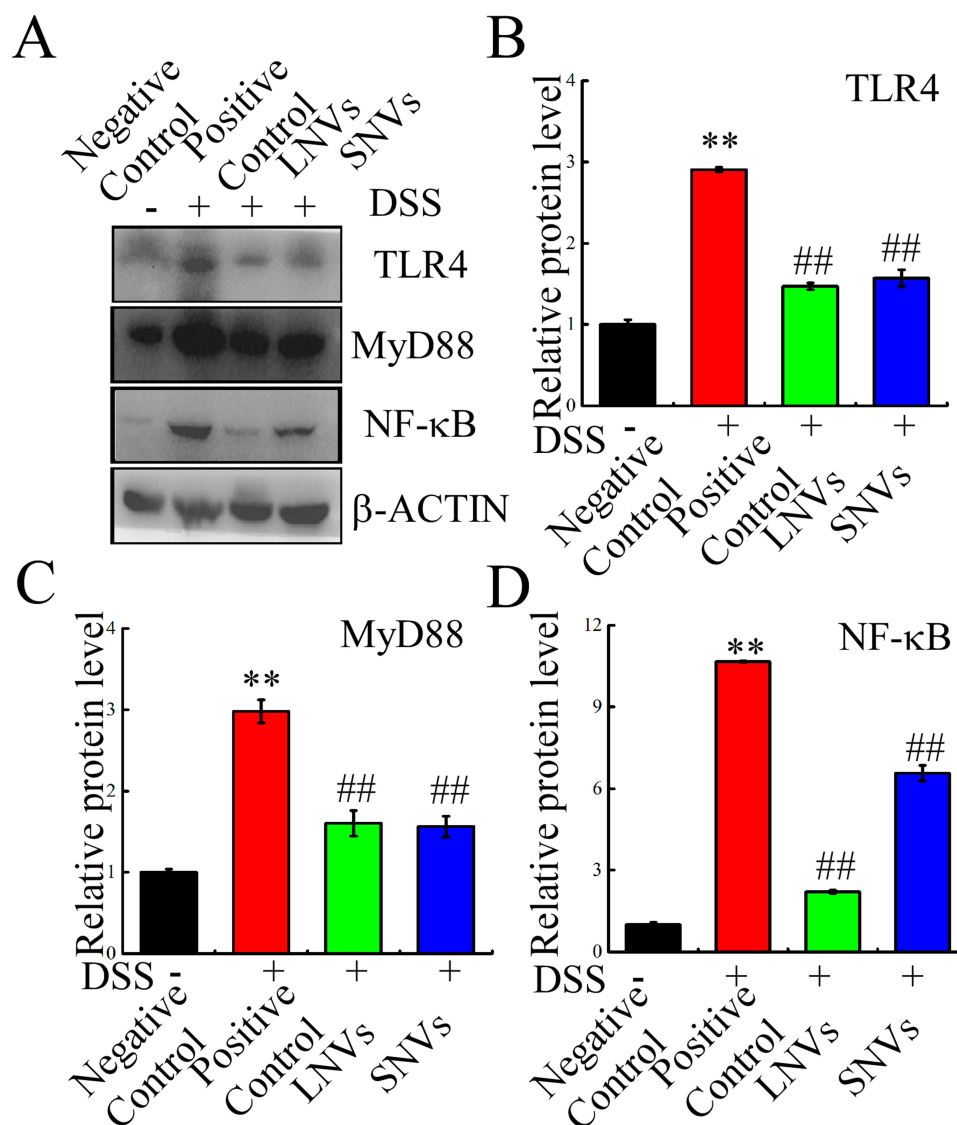


Figure 6 TcNVs suppresses the TLR4/MyD88/NF-κB signaling pathway. (A) Blots of TLR4, MyD88, p-NF-κB-p65 in the different experimental groups. (B–D) Quantification the protein levels of TLR4 (B), MyD88 (C), p-NF-κB-p65 (D) in the different experimental treatment. Error bar represents SD (n = 3). **p < 0.01 compared to the negative control group; ##p < 0.01 compared to the positive control group.

TcNVs can accumulate in large numbers in the colon when orally passed through the digestive tract (Figure 2), providing a basis for their anti-colitis activity.

Previous studies have demonstrated the pivotal role of the TLR4 signaling pathway in the inflammatory cascade during UC progression.⁴⁰ This pathway primarily mediates inflammatory responses and actively participates in immune regulation, colon inflammation, and other biological processes, thereby playing a crucial role in UC pathogenesis. In patients with chronic inflammation, disruption of the intestinal mucosal barrier leads to elevated levels of bacterial products such as LPS in the serum.⁴⁶ Upon recognition by host cells, LPS triggers activation of TLR4, subsequently initiating MyD88-dependent downstream signaling cascades. Notably, NF-κB serves as a vital transcription factor regulating immune responses, and its activation promotes synthesis of pro-inflammatory cytokines including IL-1β, IL-6, and TNF-α,¹⁴ thus significantly contributing to UC pathogenesis. In this study, administration of DSS to mice induced upregulation of TLR4 expression along with subsequent inflammatory effects consistent with findings reported by Zhu et al.¹⁵ However, our results demonstrate that TcNVs effectively suppress the expressions of TLR4, MyD88, and NF-κB as well as inhibits NF-κB-induced production of pro-inflammatory cytokines (IL-1β, IL-6, and TNF-α) within the

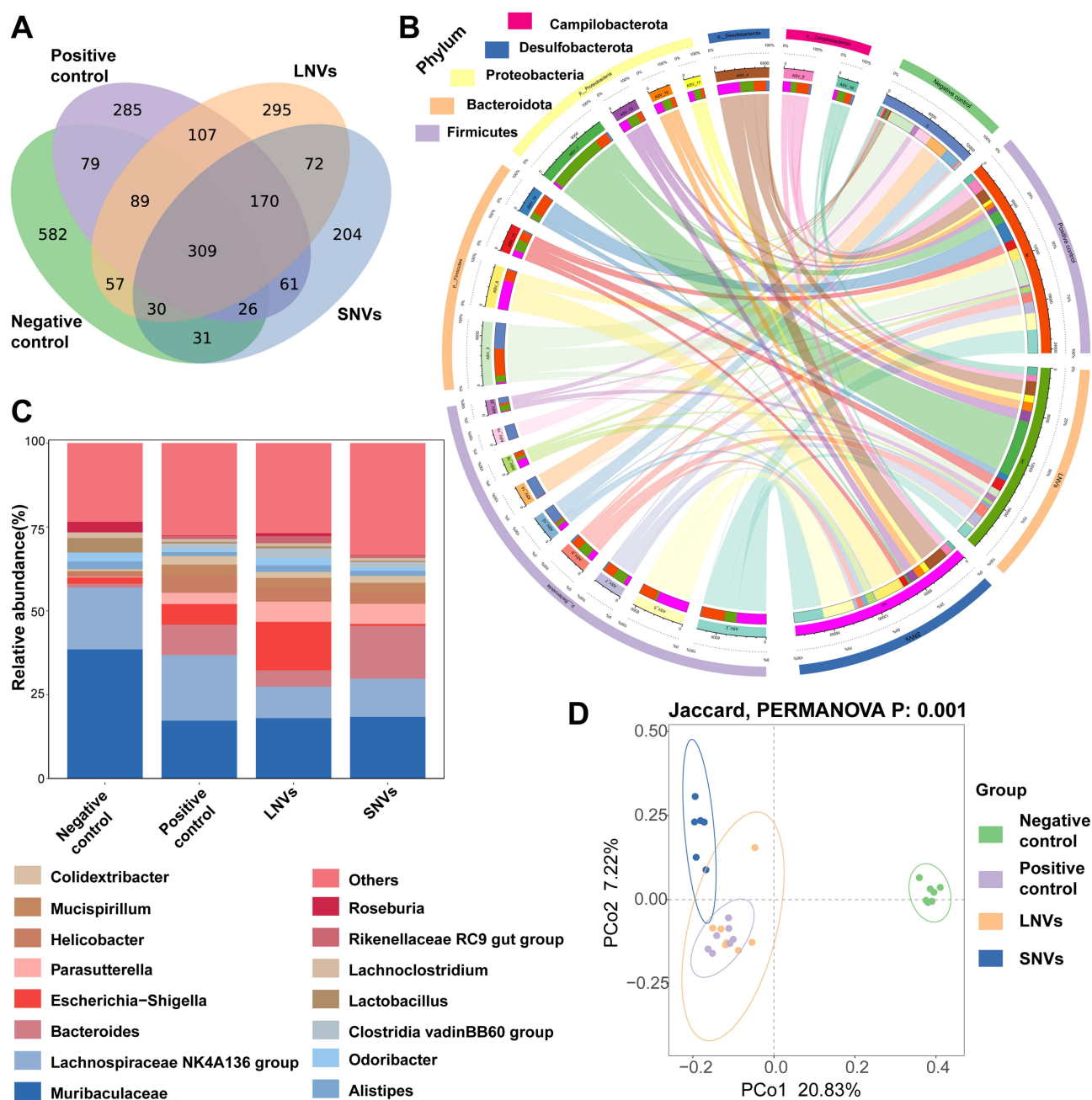
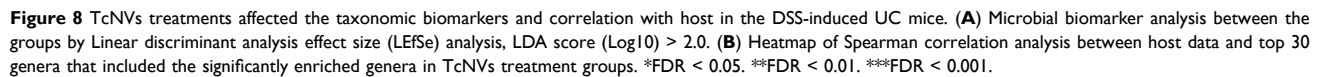


Figure 7 Change of bacterial composition and community structure of gut microbiota in DSS-induced UC mice model under TcNVs interventions. **(A)** Venn diagram of all samples from four groups at ASV level. **(B)** Circos diagram of assigned main bacterial phyla between four groups. Top five phyla were shown. **(C)** Microbial compositions at genus level between groups. Top 15 genera were shown. **(D)** Principal coordinate analysis (PCoA) of Jaccard distance for DSS-induced UC mice model with different treatments ($n = 6-7$).

colonic tissue from DSS-induced UC mice (Figures 5 and 6). These findings support that TcNVs may ameliorate colitis lesions through inhibition of TLR4/MyD88/NF- κ B signaling pathway activation.

Recent insights have increasingly implicated the microbiota residing within the gastrointestinal tract in the pathogenesis of UC.⁴⁷ Loss of homeostasis (mainly decreasing) of gut microbial diversity leads to various diseases including inflammatory bowel diseases (IBD), such as UC and Crohn's disease.⁴⁸ Generally, TcNVs (especially LNVs) presented a potential power to improve the microbial diversity disorder caused by the DSS-induced UC in mice (Figure S5). Similar to other studies, treating UC with plant-derived NVs could improve gut microbial diversity.^{15,44,49}



To further explore the Spearman correlation between alterations in intestinal microbiota and the onset of UC and the improvement effect of TcNVs on UC, we analyzed the correlation between host data (DAI, body weight, colon length), inflammatory factors (IL-1 β , IL-6, TNF- α), and intestinal microbiota. *Bacteroides* spp. which was previously indicated having an influence on the pathogenesis of the UC correlated positively with DAI and IL-6 level in our study.⁵³ Therefore, it significantly negatively correlated with colon length and body weight of mice. Genera *Muribaculaceae*, *Roseburia*, and *Lactobacillus* were found to be significantly negatively correlated with DAI and IL-6, whereas they were positively correlated with body weight of mice. It is reported that members of *Muribaculaceae* were abundant in different laboratory facilities, suggesting facility-specific emergence of this common murine gut bacteria group.⁵⁴ *Roseburia* species play a crucial role in the human gut microbiota and low levels of this bacteria have been associated with human diseases. *Lactobacillus* are considered an example of a beneficial bacterium used for probiotic-assisted therapies in IBD, where several *Lactobacillus* species were shown to mitigate gut injury as well as improve the integrity of the gut immune, epithelial layer, and bacterial vaginal membrane.⁵⁵ So, these findings again strongly support the idea that

modifying the composition of the gut microbiome appears to play an important role in decreasing the risk of developing UC.

To conclude, our work demonstrated that TcNVs not only protect macrophages from inflammation with no toxic effect *in vitro* but also meliorated DSS-induced colitis through reducing the degree of histological damage in the colon and decreasing the expression of inflammatory factors, and regulating the gut microbiota homeostasis. However, there are some limitations to this study: the need to carefully extrapolate results from animals to humans, the need to address potential microbiota gaps, differences between acute and chronic models, and so on. All these are worthy of further study by researchers.

Abbreviations

ALT, glutamic pyruvic transaminase; AST, aspartate aminotransferase; ASV, amplicon sequence variant; BCA, bicinchoninic acid; CCK-8, Cell Counting Kit-8; Cer, ceramide; Cert, phytoceramide; DAI, disease activity index; DAPI, 4',6'-diamidino-2-phenylindole; DG, diacylglycerol; DGDG, digalactosyldiacylglycerol; DGTs, diacylglyceryl trimethylhomoserine; DiR, 1,1-dioctadecyl-3,3,3,3-tetramethylindotricarbocyanine iodide; DSS, dextran sulfate sodium; ELISA, enzyme-linked immunosorbent assay; FBS, fetal bovine serum; FFA, free fatty acid; HE, hematoxylin and eosin; HexCer, hexosylceramide; IBD, inflammatory bowel diseases; IL-6, interleukin 6; LEfSe, linear discriminant analysis; LNVs, nanovesicles extracted from leaves; LPC, lysophosphatidylcholine; LPS, lipopolysaccharide; NVs, nanovesicles; PBS, phosphate buffered saline; MGDG, monogalactosyldiacylglycerol; PA, phosphatidic acid; PC, phosphatidylcholine; PCoA, Principal coordinates analysis; PCR, polymerase chain reaction; PE, phosphatidylethanolamine; PG, phosphatidylglycerol; PI, phosphatidylinositol; PMA, phorbol 12-myristate 13-acetate; PVDF, polyvinylidene difluoride; QIIME2, quantitative insights into microbial ecology 2; RPMI, Roswell Park Memorial Institute; SDS-PAGE, sodium dodecyl sulfate polyacrylamide gel electrophoresis; SNVs, nanovesicles extracted from stems; TcNVs, *Taxus chinensis*-derived nanovesicles; TG, triacylglycerol; TLR4, toll-like receptor 4; TNF, tumor necrosis factor; UC, ulcerative colitis.

Data Sharing Statement

The 16S rDNA sequencing data for all samples have been deposited in the Genome Sequence Archive database in the BIG Data Center, Chinese Academy of Sciences, under accession code CRA017176, that are accessible at <https://ngdc.cncb.ac.cn/gsa>.

Ethics Statement

All procedures in animal experiments were carried out following the guidelines approved by Ethics Committee of Southwest Jiaotong University, and all efforts were made to minimize animal suffering. The approved number was SWJTU-2503-NSFC (118).

Author Contributions

All authors made a significant contribution to the work reported, whether that is in the conception, study design, execution, acquisition of data, analysis and interpretation, or in all these areas; took part in drafting, revising or critically reviewing the article; gave final approval of the version to be published; have agreed on the journal to which the article has been submitted; and agree to be accountable for all aspects of the work.

Funding

Our work was supported by the Foundation of Sichuan Science and Technology Program (24NSFSC1611 and 2023NSFSC1844) and The Third People's Hospital of Chengdu Clinical Research Program (CSY-YN-01-2023-065 and CSY-YN-03-2024-015).

Disclosure

The authors declare no conflicts of interest in this work.

References

- Cantoro L, Monterubbianesi R, Falasco G, et al. The earlier you find, the better you treat: red flags for early diagnosis of inflammatory bowel disease. *Diagnostics*. **2023**;13(20):3183. doi:10.3390/diagnostics13203183
- Upadhyay KG, Desai DC, Ashavaid TF, Dherai AJ. Microbiome and metabolome in inflammatory bowel disease. *J Gastroenterol Hepatol*. **2023**;38(1):34–43. doi:10.1111/jgh.16043
- Zhang W, Michalowski CB, Belouqui A. Oral delivery of biologics in inflammatory bowel disease treatment. *Front Bioeng Biotechnol*. **2021**;9:675194. doi:10.3389/fbioe.2021.675194
- Hanauer SB. New steroids for IBD: progress report. *Gut*. **2002**;51:182–183. doi:10.1136/gut.51.2.182
- Zeng Z, He X, Li C, et al. Oral delivery of antioxidant enzymes for effective treatment of inflammatory disease. *Biomaterials*. **2021**;271:120753. doi:10.1016/j.biomaterials.2021.120753
- Han W, Xie B, Li Y, et al. Orally deliverable nanotherapeutics for the synergistic treatment of colitis-associated colorectal cancer. *Theranostics*. **2019**;9(24):7458–7473. doi:10.7150/thno.38081
- Zhang M, Xu C, Liu D, Han MK, Wang L, Merlin D. Oral delivery of nanoparticles loaded with ginger active compound, 6-shogaol, attenuates ulcerative colitis and promotes wound healing in a murine model of ulcerative colitis. *J Crohns Colitis*. **2018**;12(2):217–229. doi:10.1093/ecco-jcc/jjx115
- Liu P, Gao C, Chen H, et al. Receptor-mediated targeted drug delivery systems for treatment of inflammatory bowel disease: opportunities and emerging strategies. *Acta Pharm Sin B*. **2021**;11(9):2798–2818. doi:10.1016/j.apsb.2020.11.003
- Xu Z, Xu Y, Zhang K, et al. Plant-derived extracellular vesicles (PDEVs) in nanomedicine for human disease and therapeutic modalities. *J Nanobiotechnology*. **2023**;21(1):114. doi:10.1186/s12951-023-01858-7
- Feng J, Xiu Q, Huang Y, Troyer Z, Li B, Zheng L. Plant-derived vesicle-like nanoparticles as promising biotherapeutic tools: present and future. *Adv Mater*. **2023**;35(24):e2207826. doi:10.1002/adma.202207826
- Cao M, Diao N, Cai X, et al. Plant exosome nanovesicles (PENs): green delivery platforms. *Mater Horiz*. **2023**;10(10):3879–3894. doi:10.1039/D3MH01030A
- Simons M, Raposo G. Exosomes—vesicular carriers for intercellular communication. *Curr Opin Cell Biol*. **2009**;21(4):575–581.
- Ju S, Mu J, Dokland T, et al. Grape exosome-like nanoparticles induce intestinal stem cells and protect mice from DSS-induced colitis. *Mol Ther*. **2013**;21(7):1345–1357. doi:10.1038/mt.2013.64
- Liu C, Yan X, Zhang Y, et al. Oral administration of turmeric-derived exosome-like nanovesicles with anti-inflammatory and pro-resolving bioactions for murine colitis therapy. *J Nanobiotechnology*. **2022**;20(1):206. doi:10.1186/s12951-022-01421-w
- Zhu Z, Liao L, Gao M, Liu Q. Garlic-derived exosome-like nanovesicles alleviate dextran sulphate sodium-induced mouse colitis via the TLR4/MyD88/NF- κ B pathway and gut microbiota modulation. *Food Funct*. **2023**;14(16):7520–7534. doi:10.1039/D3FO01094E
- Gong Q, Xiong F, Zheng Y, Guo Y. Tea-derived exosome-like nanoparticles prevent irritable bowel syndrome induced by water avoidance stress in rat model. *J Gastroenterol Hepatol*. **2024**;39(12):2690–2699. doi:10.1111/jgh.16714
- Sriwastva MK, Deng ZB, Wang B, et al. Exosome-like nanoparticles from Mulberry bark prevent DSS-induced colitis via the AhR/COPS8 pathway. *EMBO Rep*. **2022**;23(3):e53365. doi:10.15252/embr.202153365
- Gong Q, Zeng Z, Jiang T, et al. Anti-fibrotic effect of extracellular vesicles derived from tea leaves in hepatic stellate cells and liver fibrosis mice. *Front Nutr*. **2022**;9:1009139. doi:10.3389/fnut.2022.1009139
- Wani MC, Taylor HL, Wall ME, Coggon P, McPhail AT. Plant antitumor agents. VI. The isolation and structure of taxol, a novel antileukemic and antitumor agent from *Taxus brevifolia*. *J Am Chem Soc*. **1971**;93(9):2325–2327. doi:10.1021/ja00738a045
- Rowinsky EK, Cazenave LA, Donehower RC. Taxol: a novel investigational antimicrotubule agent. *J Natl Cancer Inst*. **1990**;82(15):1247–1259. doi:10.1093/jnci/82.15.1247
- Gallego-Jara J, Lozano-Terol G, Sola-Martínez RA, Cánovas-Díaz M, De Diego Puente T. A compressive review about Taxol®: history and future challenges. *Molecules*. **2020**;25(24):5986. doi:10.3390/molecules25245986
- Slichenmyer WJ, Von Hoff DD. Taxol: a new and effective anti-cancer drug. *Anticancer Drugs*. **1991**;2(6):519–530. doi:10.1097/00001813-199112000-00002
- Iiyama S, Fukaya K, Yamaguchi Y, et al. Total synthesis of paclitaxel. *Org Lett*. **2022**;24(1):202–206. doi:10.1021/acs.orglett.1c03851
- Petrini O, Sieber TN, Toti L, Viret O. Ecology, metabolite production, and substrate utilization in endophytic fungi. *Nat Toxins*. **1992**;1:185–196. doi:10.1002/nt.2620010306
- Zhang S, Lu X, Zheng T, Guo X, Chen Q, Tang Z. Investigation of bioactivities of *Taxus chinensis*, *Taxus cuspidata*, and *Taxus × media* by gas chromatography-mass spectrometry. *Open Life Sci*. **2021**;16(1):287–296. doi:10.1515/biol-2021-0032
- Yamawaki C, Oyama M, Yamaguchi Y, Ogita A, Tanaka T, Fujita KI. Curcumin potentiates the fungicidal effect of dodecanol by inhibiting drug efflux in wild-type budding yeast. *Lett Appl Microbiol*. **2019**;68(1):17–23. doi:10.1111/lam.13083
- Dijkmans AC, Zacarias NVO, Burggraaf J, et al. Fosfomycin: pharmacological, clinical and future perspectives. *Antibiotics*. **2017**;6(4):24. doi:10.3390/antibiotics6040024
- Hronská H, Tokořová S, Pilníková A, Křiřtířková Ľ, Rosenberg M. Bioconversion of fumaric acid to L-malic acid by the bacteria of the genus *Nocardia*. *Appl Biochem Biotechnol*. **2015**;175(1):266–273. doi:10.1007/s12010-014-1251-1
- Saffari VR, Saffari M. Effects of EDTA, citric acid, and tartaric acid application on growth, phytoremediation potential, and antioxidant response of *Calendula officinalis* L. in a cadmium-spiked calcareous soil. *Int J Phytoremediation*. **2020**;22(11):1204–1214. doi:10.1080/15226514.2020.1754758
- Maurya DK, Devasagayam TP. Antioxidant and prooxidant nature of hydroxycinnamic acid derivatives ferulic and caffeic acids. *Food Chem Toxicol*. **2010**;48(12):3369–3373. doi:10.1016/j.fct.2010.09.006
- Ward JL, Wu Y, Harflett C, et al. Miyabeacin: a new cyclodimer presents a potential role for willow in cancer therapy. *Sci Rep*. **2020**;10(1):6477. doi:10.1038/s41598-020-63349-1
- Bolyen E, Rideout JR, Dillon MR, et al. Reproducible, interactive, scalable and extensible microbiome data science using QIIME 2. *Nat Biotechnol*. **2019**;37(8):852–857. doi:10.1038/s41587-019-0209-9
- Rome S. Biological properties of plant-derived extracellular vesicles. *Food Funct*. **2019**;10(2):529–538. doi:10.1039/C8FO02295J

34. Jung D, Kim NE, Kim S, et al. Plant-derived nanovesicles and therapeutic application. *Pharmacol Ther.* 2025;269:108832. doi:10.1016/j.pharmthera.2025.108832
35. Oskouie MN, Aghili Moghaddam NS, Butler AE, Zamani P, Sahebkar A. Therapeutic use of curcumin-encapsulated and curcumin-primed exosomes. *J Cell Physiol.* 2019;234(6):8182–8191. doi:10.1002/jcp.27615
36. Zu M, Xie D, Canup BSB, et al. ‘Green’ nanotherapeutics from tea leaves for orally targeted prevention and alleviation of colon diseases. *Biomaterials.* 2021;279:121178. doi:10.1016/j.biomaterials.2021.121178
37. Zhao H, Cheng N, Zhou W, et al. Honey polyphenols ameliorate DSS-induced ulcerative colitis via modulating gut microbiota in rats. *Mol Nutr Food Res.* 2019;63(23):e1900638. doi:10.1002/mnfr.201900638
38. Yang C, Zhang M, Lama S, Wang L, Merlin D. Natural-lipid nanoparticle-based therapeutic approach to deliver 6-shogaol and its metabolites M2 and M13 to the colon to treat ulcerative colitis. *J Control Release.* 2020;323:293–310. doi:10.1016/j.jconrel.2020.04.032
39. Wang Z, Li S, Cao Y, et al. Oxidative stress and carbonyl lesions in ulcerative colitis and associated colorectal cancer. *Oxid Med Cell Longev.* 2016;2016:9875298. doi:10.1155/2016/9875298
40. Zhou J, Tan L, Xie J, et al. Characterization of brusatol self-microemulsifying drug delivery system and its therapeutic effect against dextran sodium sulfate-induced ulcerative colitis in mice. *Drug Deliv.* 2017;24(1):1667–1679. doi:10.1080/10717544.2017.1384521
41. Lee SH, Bajracharya R, Min JY, Han JW, Park BJ, Han HK. Strategic approaches for colon targeted drug delivery: an overview of recent advancements. *Pharmaceutics.* 2020;12(1):68. doi:10.3390/pharmaceutics12010068
42. Zhang M, Merlin D. Nanoparticle-based oral drug delivery systems targeting the colon for treatment of ulcerative colitis. *Inflamm Bowel Dis.* 2018;24(7):1401–1415. doi:10.1093/ibd/izy123
43. Sundaram K, Miller DP, Kumar A, et al. Plant-derived exosomal nanoparticles inhibit pathogenicity of porphyromonas gingivalis. *iScience.* 2020;23(2):100869. doi:10.1016/j.isci.2020.100869
44. Gao C, Zhou Y, Chen Z, et al. Turmeric-derived nanovesicles as novel nanobiologics for targeted therapy of ulcerative colitis. *Theranostics.* 2022;12(12):5596–5614. doi:10.7150/thno.73650
45. Gong Q, Sun Y, Liu L, Pu C, Guo Y. Oral administration of tea-derived exosome-like nanoparticles protects epithelial and immune barrier of intestine from psychological stress. *Heliyon.* 2024;10(17):e36812. doi:10.1016/j.heliyon.2024.e36812
46. Pasternak BA, D’Mello S, Jurickova II, et al. Lipopolysaccharide exposure is linked to activation of the acute phase response and growth failure in pediatric Crohn’s disease and murine colitis. *Inflamm Bowel Dis.* 2010;16(5):856–869. doi:10.1002/ibd.21132
47. Nishida A, Inoue R, Inatomi O, Bamba S, Naito Y, Andoh A. Gut microbiota in the pathogenesis of inflammatory bowel disease. *Clin J Gastroenterol.* 2018;11(1):1–10. doi:10.1007/s12328-017-0813-5
48. Zhang Y, Si X, Yang L, Wang H, Sun Y, Liu N. Association between intestinal microbiota and inflammatory bowel disease. *Animal Model Exp Med.* 2022;5(4):311–322. doi:10.1002/ame2.12255
49. Li J, Luo T, Wang D, et al. Therapeutic application and potential mechanism of plant-derived extracellular vesicles in inflammatory bowel disease. *J Adv Res.* 2024;68:63–74.
50. Pilarczyk-Zurek M, Strus M, Adamski P, Hezko PB. The dual role of Escherichia coli in the course of ulcerative colitis. *BMC Gastroenterol.* 2016;16(1):128. doi:10.1186/s12876-016-0540-2
51. Bai D, Zhao J, Wang R, et al. Eubacterium coprostanoligenes alleviates chemotherapy-induced intestinal mucositis by enhancing intestinal mucus barrier. *Acta Pharm Sin B.* 2024;14(4):1677–1692. doi:10.1016/j.apsb.2023.12.015
52. Aden K, Rehman A, Waschina S, et al. Metabolic functions of gut microbes associate with efficacy of tumor necrosis factor antagonists in patients with inflammatory bowel diseases. *Gastroenterology.* 2019;157(5):1279–1292. doi:10.1053/j.gastro.2019.07.025
53. Lucke K, Miehke S, Jacobs E, Schuppler M. Prevalence of Bacteroides and Prevotella spp. in ulcerative colitis. *J Med Microbiol.* 2006;55(Pt 5):617–624. doi:10.1099/jmm.0.46198-0
54. Bowerman KL, Knowles SCL, Bradley JE, et al. Effects of laboratory domestication on the rodent gut microbiome. *ISME Commun.* 2021;1(1):49. doi:10.1038/s43705-021-00053-9
55. Li C, Peng K, Xiao S, Long Y, Yu Q. The role of Lactobacillus in inflammatory bowel disease: from actualities to prospects. *Cell Death Discov.* 2023;9(1):361. doi:10.1038/s41420-023-01666-w